1956

Frequency response of nonlinear servomechanisms

Swift, Douglas D.

Monterey, California. Naval Postgraduate School

FREQUENCY RESPONSE OF NONLINEAR SERVOMECHANISMS

Enrique F. Gutierrez

and

Douglas D. Swift

FREQUENCY RESPONSE
OF
NONLINEAR SERVOMECHANISMS

* * * * *

Enrique F. Gutiérrez

and

Douglas D. Swift

FREQUENCY RESPONSE OF

NONLINEAR SERVOMECHANISMS

by

Enrique F. Gutiérrez
Lieutenant, Chilean Navy

and

Douglas D. Swift
Lieutenant, United States Navy

Submitted in partial fulfillment
of the requirements
for the degree of
MASTER OF SCIENCE
IN
ELECTRICAL ENGINEERING

United States Naval Postgraduate School
Monterey, California

1 9 5 6

This work is accepted as fulfilling

the thesis requirements for the degree of

MASTER OF SCIENCE

IN

ELECTRICAL ENGINEERING

from the

United States Naval Postgraduate School

PREFACE

Transient response characteristics are essential to the design of servomechanisms. In linear systems there is direct correlation between frequency response and transient response,[1] but this correlation does not exist in nonlinear systems. From a study of the frequency response of nonlinear systems, however, certain predictions may be made as to the transient response.

In conducting laboratory work on a two phase motor servo it was noted that the frequency response of both a single and double loop system was dependent on the test signal amplitude. Investigation revealed that this is well known, but not adequately explained. From a study of the literature[2] it was conceivable that the frequency response of nonlinear systems might be obtained in terms of linear differential equation theory using concepts of variable gain and time constants. This is developed in the following thesis.

This work was conducted at the United States Naval Postgraduate School during the period August 1955 to May 1956.

The authors acknowledge the assistance of the faculty of the Department of Electrical Engineering and in particular the guidance of Professor G. J. Thaler.

TABLE OF CONTENTS

LIST OF ILLUSTRATIONS

TABLE OF SYMBOLS

θ_A	Analyzer (tester) input signal (a voltage)
θ_c	Output position of load (a voltage)
θ_R	Command signal (a voltage)
τ_m	Time constant of motor-load combination
ω	Frequency (radians/second)
A,B,C	Constants
E	A voltage
f	Viscous friction factor
g	Equivalent damping coefficient
J	Equivalent moment of inertia
K	A constant
K_1	Error signal gain constant
K_3	$K_s/K_{CT}N$
K_A	Amplifier gain constant
K_{CT}	Control transformer constant
K_E	Output signal potentiometer setting
K_m	Gain constant of the motor-load combination
K_s	Tachometer constant
K_t	Tachometer signal potentiometer setting
K_{tr}	Transformer ratio, input/output
L	Length (a dimension)
M	Mass (a dimension)
R	Resistance
S	Speed in radians/second
T	Time (a dimension)

T_o	Torque
V_c	Control field voltage
V_L	Line voltage
V_{ref}	Reference field voltage
V_s	Tachometer voltage component due to speed of tachometer
V_t	Tachometer voltage component due to transformer action
V_{tach}	Tachometer output voltage
Y	Admittance

CHAPTER I

THE PROBLEM

1. Introduction.

The purpose of this study is the analysis of a simple positioning servomechanism using a two phase servomotor and including the nonlinear effects produced by the motor itself. In order to analyze the effect of the nonlinearity it is assumed that the results previously obtained[2] are essentially correct; i. e., the motor-load combination can be expressed by a transfer function of normal algebraic form in which the gain constant symbol and the time constant symbol represent parameters which are characteristic of the motor.

Starting with this assumption it is possible to manipulate the transfer function equations into various algebraic forms, maintaining the identity of the nonlinear quantities. Methods are then developed which permit analytical or graphical interpretation of these equations including the effect of the nonlinear parameters. In order to carry out an intelligent analysis and in order to verify the results of such analysis, a specific physical system was assembled and tested, from which values characteristic of the motor parameters were obtained. These values are used in computing the frequency response of the nonlinear system for specific test conditions using methods developed in this thesis. These computations are verified experimentally with care taken to duplicate the conditions specified in the mathematical computations.

Comparison of the experimental and computed results indicates that the effects of the nonlinearities are adequately predicted by the computational

techniques. It is felt that these methods are applicable to design procedures when it is necessary to consider the nonlinearity of the two phase motor.

2. The system.

The servomechanism under study is typical of simple positioning systems and is diagrammed in Figure 1. This system was operated and analyzed both as a single loop system with only error signal feedback and as a double loop system with derivative (tachometer) feedback.

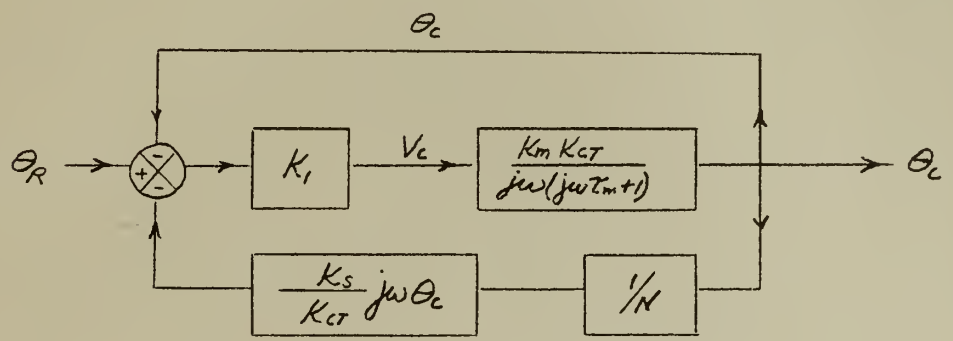

Figure 1. Typical positioning servomechanism

First, consider this to be a linear system; i. e., the gain constant (K_m) and time constant (τ_m) of the motor-load combination are actually constant. For the sake of simplicity the following equations are first presented for a single loop system and will be extended later for a double loop system.

From the block diagram it is found that:

$$\theta_c = \frac{K_m K_{cT}}{j\omega(j\omega\tau_m+1)} V_c \qquad (1)$$

$$\frac{\theta_c}{|\theta_R|} \qquad \frac{K_m K_{CT}}{j\omega(j\omega\tau_m+1)} \qquad \frac{V_c}{|\theta_R|} \tag{1a}$$

$$\frac{\theta_c}{\theta_R-\theta_c} = KG = \frac{K_1\theta_c}{V_c} \qquad \frac{K_1 K_m K_{CT}}{j\omega(j\omega\tau_m+1)} \tag{2}$$

$$\frac{\theta_c}{\theta_R} = \frac{KG}{1+KG} = \frac{\dfrac{K_1 K_m K_{CT}}{j\omega(j\omega\tau_m+1)}}{1+\dfrac{K_1 K_m K_{CT}}{j\omega(j\omega\tau_m+1)}} \tag{3}$$

From equations (1a) and (3) it is seen that:

$$\left|\frac{\theta_c}{\theta_R}\right| = \frac{K_m K_{CT}}{\omega\sqrt{\omega^2\tau_m^2+1}} \quad \frac{|V_c|}{|\theta_R|} \tag{4}$$

$$\frac{\theta_c}{\theta_R} = \frac{K_1 K_m K_{CT}}{\sqrt{(K_1 K_m K_{CT}-\omega^2\tau_m)^2+\omega^2}} \tag{5}$$

$$\tan\angle\frac{\theta_c}{\theta_R} = \frac{-\omega}{K_1 K_m K_{CT}-\omega^2\tau_m} \tag{6}$$

These equations are derived in Appendix A.

For a linear system the relations expressed in equations (4), (5) and (6) are unique, since the quantities K_m, K_{CT} and τ_m, which are characteristics of the system, are constant.

Now consider this same system as described in Figure 1 to be nonlinear; that is, the "time constant" (τ_m) and "gain constant" (K_m) are variables which are characteristics of the motor. A unique frequency response no longer exists for this nonlinear system since the frequency response function is dependent on the magnitude of the disturbing signal θ_R.

It is necessary to specify the test condition for which the frequency response is to be measured or calculated. Equation (4) indicates that there are three conditions of interest. These conditions are:

a. Sinusoidal input of constant specified magnitude.

b. Periodic output of constant specified magnitude.

c. Periodic control field voltage of constant specified magnitude.

The frequency response of a nonlinear system under any of these conditions may be obtained from the steady state solution of the nonlinear differential equations of the system. Although the mathematical solutions of these equations must exist, they have not yet been found, and some means of approaching the solutions are desirable.

The nonlinearity of the system is primarily due to variation in the parameters called "gain constant" and "time constant". It has been shown[2] that these "constants" can be thought to be functions of the control field voltage, V_c, and can be measured experimentally as well as computed from the torque vs. speed curves. Knowing the functions relating K_m and τ_m to V_c, the above equations can be solved simultaneously in terms of V_c as a parameter to determine the frequency response for any specified condition.

The equations given above may be extended to include derivative feedback (two loop system). Equations (1) and (4) remain unchanged. The frequency response, equation (3), is changed to:

$$\frac{\theta_c}{\theta_R} = \frac{\dfrac{K_1 K_m K_{cT}}{j\omega(j\omega\tau_m+1)}}{1 + \dfrac{K_1 K_m K_{cT}}{j\omega(j\omega\tau_m+1)}(1+j\omega k_3)} \qquad (7)$$

where $AF = (1+j\omega k_3)$ and $k_3 = \dfrac{k_s}{K_{cT} N}$ from the block diagram. (8)

From equation (7) the magnitude ratio and the phase angle are easily found to be:

$$\left|\frac{\theta_c}{\theta_R}\right| = \frac{K_1 K_m K_{CT}}{\sqrt{(K_1 K_m K_{CT} - \omega^2 \tau_m)^2 + \omega^2 (1 + K_1 K_m K_{CT} K_3)^2}} \tag{9}$$

$$\tan \angle \frac{\theta_c}{\theta_R} = \frac{-\omega (1 + K_1 K_m K_{CT} K_3)}{K_1 K_m K_{CT} - \omega^2 \tau_m} \tag{10}$$

In order that the extension of linear theory to nonlinear systems be valid, it must be assumed that values of K_m and τ_m exist such that these relations apply, and these values of K_m and τ_m are functions of V_c. If this is true, the solutions of the above equations may be performed in three ways: by maintaining constant θ_R, θ_c, or V_c. The details of these solutions by both analytical and graphical methods is the subject of Chapter II, III and IV. The existence and measurement of K_m and τ_m such that these relations are valid is discussed in Chapter V.

CHAPTER II

SOLUTION BY CONSTANT INPUT SIGNAL

Servomechanisms are generally tested by maintaining a sinusoid of constant amplitude for a test signal (which is proportional to θ_R) and observing the output as a function of the test signal frequency. Eliminating $\left|\frac{\theta_c}{\theta_R}\right|$ in equations (4) and (9):

$$\tau_m^2\left(K_1^2-\left|\frac{V_c}{\theta_R}\right|^2\right)\omega^4+\left[K_1^2-\left|\frac{V_c}{\theta_R}\right|^2+2K_1K_mK_{CT}\left|\frac{V_c}{\theta_R}\right|^2\tau_m\right.$$

$$\left.-K_1^2K_3^2K_m^2K_{CT}^2\left|\frac{V_c}{\theta_R}\right|^2-2K_1K_3K_mK_{CT}\left|\frac{V_c}{\theta_R}\right|^2\right]\omega^2-K_1^2K_m^2K_{CT}^2\left|\frac{V_c}{\theta_R}\right|^2=0 \quad (11)$$

which is of the form

$$A\omega^4+B\omega^2+C=0 \quad (12)$$

from which one may obtain zero, one, or two real, positive solutions for ω, depending on the signs and magnitudes of the coefficients. This is in agreement with the physical considerations of the system. In the following discussion the word "solution" is construed to mean "real, positive solution" except where otherwise noted.

As discussed in Chapter V, for a given sinusoidal V_c of constant amplitude unique numerical values may be given to K_m and τ_m. By varying the parameter V_c, it is seen that for low values of $\left|\frac{V_c}{\theta_R}\right|$ only one solution is possible, and as V_c is increased a point is reached where two solutions are obtained, continuing until V_c reaches a value where $B^2 - 4AC$ is zero, and the two solutions are equal. Beyond this point V_c can no longer be physically increased (the solution of equation (11) is complex). This may also be stated that as the frequency is increased, V_c increases until some maximum value is obtained, beyond which V_c decreases with

further increase in frequency. As the frequency approaches infinity, V_c tends to a value where A = 0 in equation (12), which corresponds to $V_c = K_1\theta_R$. This is easily verified experimentally.

On semilog paper the resulting frequency response curve appears as is shown in Figure 2, where the curves of $\left|\frac{\theta_c}{\theta_R}\right|$ for constant V_c are the asymptotic plots of equation (1a).

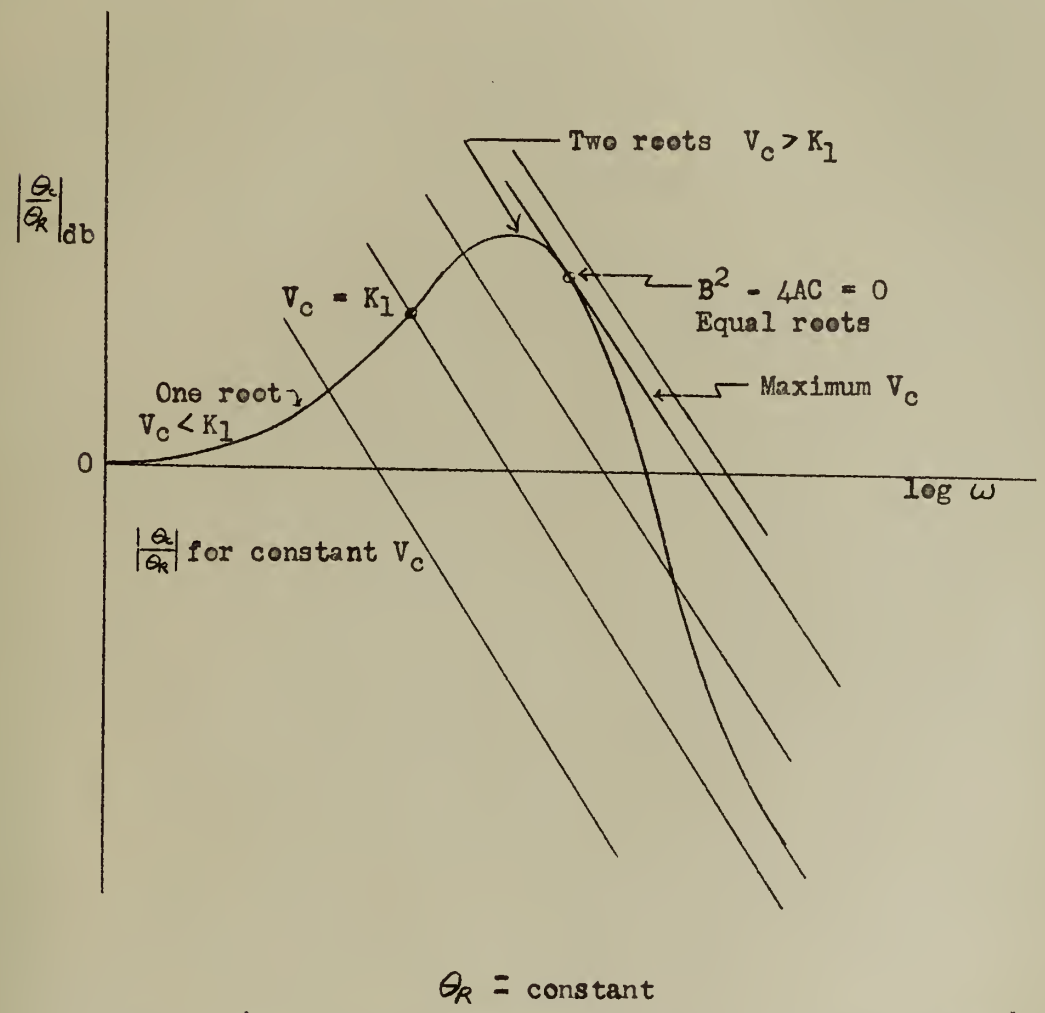

θ_R = constant

Figure 2. Frequency response curve for nonlinear system.

Remembering that θ_R is constant in amplitude, the solution is analytically obtained as follows:

1. Pick a value of V_c, starting with low values.

2. From the curve of K_m and τ_m vs. V_c, as discussed in Chapter V, pick the corresponding values of K_m and τ_m.

3. Solve for ω from equation (11) and for $\left|\frac{\theta_c}{\theta_R}\right|$ and the angle from equations (4) or (9) and (6) or (10), respectively.

4. Increase V_c by steps until $B^2 - 4AC = 0$, obtaining as many points as desired. The increment of V_c is very critical near the resonance point.

If a digital computer is available, the system response under a great number of conditions may be rapidly solved. K_m and τ_m may be inserted in the program either as a table look-up or by fitting an equation to the curves of K_m and τ_m vs. V_c.

Obviously, a simultaneous solution of equations (1a) and (3) or (7), as the case may be, may be obtained graphically. A procedure has been devised by which both the phase and magnitude of equation (7) may be obtained from equation (2)[3,4]. The intersection of the magnitude portion of this curve of equation (7) and a curve of equation (4) determines a point (or points, since two may exist) on the magnitude of the frequency response curve for constant θ_R, and for that particular value of V_c.

The phase of θ_c with respect to θ_R is given by the phase of equation (7) at the intersection frequency.

It is to be noted that equation (4) may be obtained by multiplying the magnitude of equation (2) by the constant $\frac{1}{K_1} \times \left|\frac{V_c}{\theta_R}\right|$.

One of the methods for graphically determing these points utilizes the Nichols procedure. Specifically, the procedure without tachometer feedback is:

1. For a specific V_c draw the Bode diagram of equation (2).

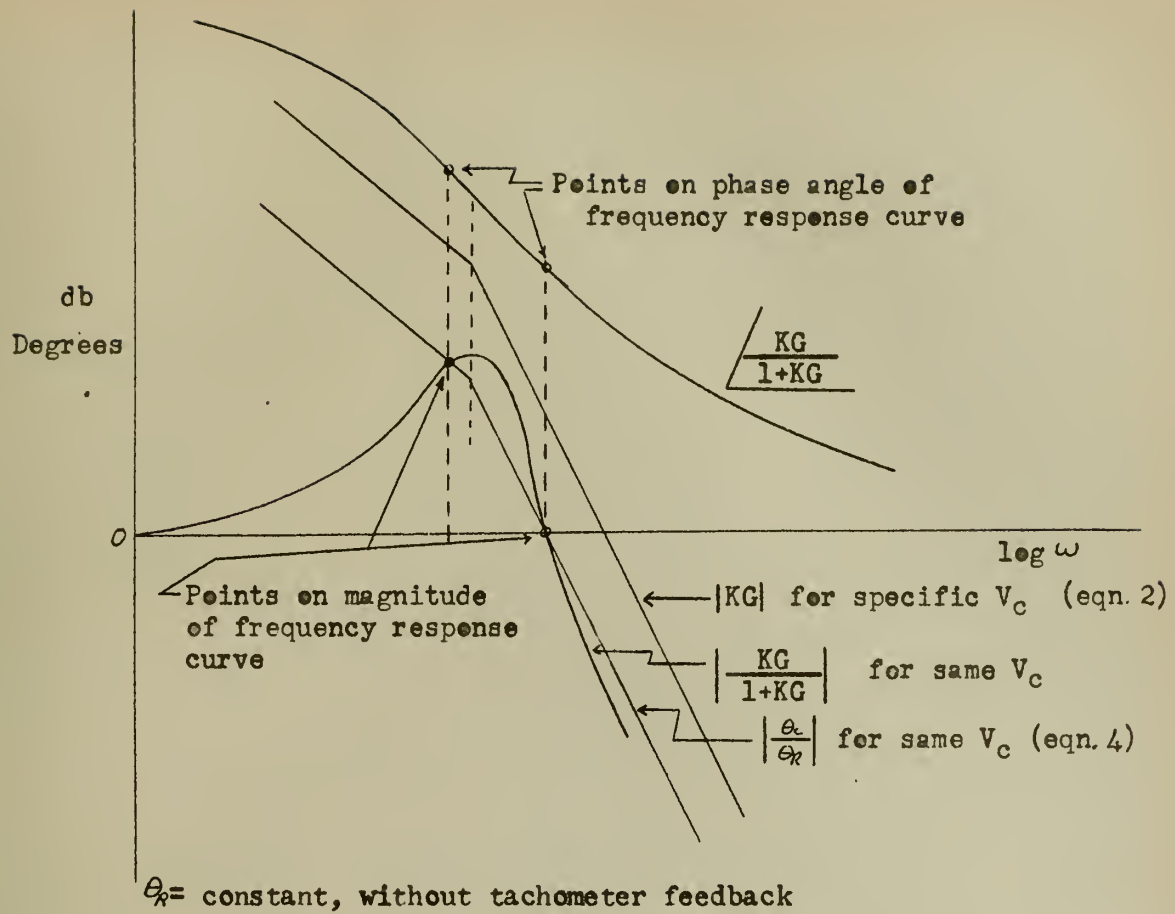

Figure 3, Construction of frequency response curve.

2. By the Nichols procedure obtain a plot of $\frac{KG}{1+KG}$ on decibel vs. log ω coordinates.

3. Superpose on the curve obtained in step 2 a plot of equation (4) for the chosen V_c. The intersection (or intersections) of this curve and magnitude curve obtained in step 2 is a point (or points) on the frequency response curve of the system. The plot of equation (4) is easily obtained from step 1 by displacing the magnitude curve of KG a number of decibels corresponding to $\frac{1}{K_1} \times \left|\frac{V_c}{\theta_R}\right|$ with proper sign.

4. The phase angle of the response is given by the phase obtained in step 2 for the intersection frequency.

Repeat this procedure for various values of V_c, obtaining as many points as desired. The graphical method is illustrated in Figure 3.

When tachometer feedback is used this procedure is modified by replacing KG by KGAF in step 1, where from equation (7):

$$KGAF = \frac{K_1 K_m K_{cr} (j\omega K_3 + 1)}{j\omega(j\omega\tau_m + 1)} \tag{13}$$

determining, in step 2, a curve of

$$\frac{KGAF}{1 + KGAF} .$$

To obtain a plot of $\frac{KG}{1+KGAF}$ add the following step:

5. Plot the Bode diagram of $AF = (j\omega K_3 + 1)$ and subtract from the points obtained in steps 3 and 4 for the magnitude (in db) and phase angle respectively. It is noted that AF is independent of the control field voltage.

With or without tachometer feedback this method is rather tedious and the analytical solution is recommended.

CHAPTER III

SOLUTION BY CONSTANT OUTPUT SIGNAL

In the study of the frequency response of a servomechanism, one is primarily interested in the magnitude ratio of output to input as a function of frequency, and secondarily as a function of the control field voltage. It seems logical, then, to consider the output to be constant and determine the value of input necessary to give this output at various frequencies. In a normal test setup, these conditions are readily obtained using a Millman adder circuit[5] input rather than the series input. A series input may be used if the test signal is properly amplified.

Solving equation (4) for ω^2,

$$\omega^2 = \frac{-1 \pm \sqrt{1 + \left(\frac{2K_m K_{cr} |V_c| \tau_m}{|\theta_c|}\right)^2}}{2\tau_m^2} \qquad (14)$$

for which only one real positive solution of ω exists and a solution exists for all values of θ_c and V_c.

The analytical procedure for a fixed value of θ_c is:

1. Pick a value of V_c, starting with low values.
2. Obtain the corresponding values of K_m and τ_m for this V_c.
3. Solve for ω in equation (14).
4. With this value of ω solve equations (5) and (6) or (9) and (10), as the case may be, for the ratio $\left|\frac{\theta_c}{\theta_R}\right|$ and the angle respectively.
5. Increase the value of the control field voltage by steps, obtaining as many points as desired. Again, the values of V_c are critical near the resonance point.

Although a real, positive solution of equation (14) exists for all values of V_c and θ_c , analysis of equation (5) and (9) reveals that as ω increases the magnitude ratio follows the familiar frequency response pattern.

For a particular value of V_c, equation (14) may be solved graphically by plotting the magnitude of equation (1). The intersection of this curve with a curve of the equation θ_c = constant yields a value of ω which satisfies both of these equations. Substituting this value of ω into equation (7) yields a point on the frequency response curve, both magnitude and phase, for this value of V_c. This appears to be a rather involved method of obtaining individual points on the frequency response, but the nicety of graphical solution, utilizing the Nichols procedure[3,4], is indicated below.

For a constant θ_c and without derivative (tachometer) feedback, one method for graphical solution is as follows:

1. Construct asymptotic plots of equation (1) for different values of control field voltage, V_c, the magnitude appearing as straight line segments as shown in Figure 4.

2. Draw a horizontal line on this diagram for the chosen value of θ_c obtaining points 1, 2, 3,....

3. Displace each of these points a distance corresponding to $\frac{K_1}{V_c}$ (in db) obtaining points 1', 2', 3',..., resulting in a curve of $KG = \frac{K_1 \theta_c}{V_c}$, which is equation (1a), and whose phase is given by the phase of step 1 for these intersection frequencies.

4. The response curve may now be obtained by the Nichols procedure resulting in

$$\frac{\theta_c}{\theta_R} = \frac{KG}{1+KG}$$

which will appear as shown in Figure 4.

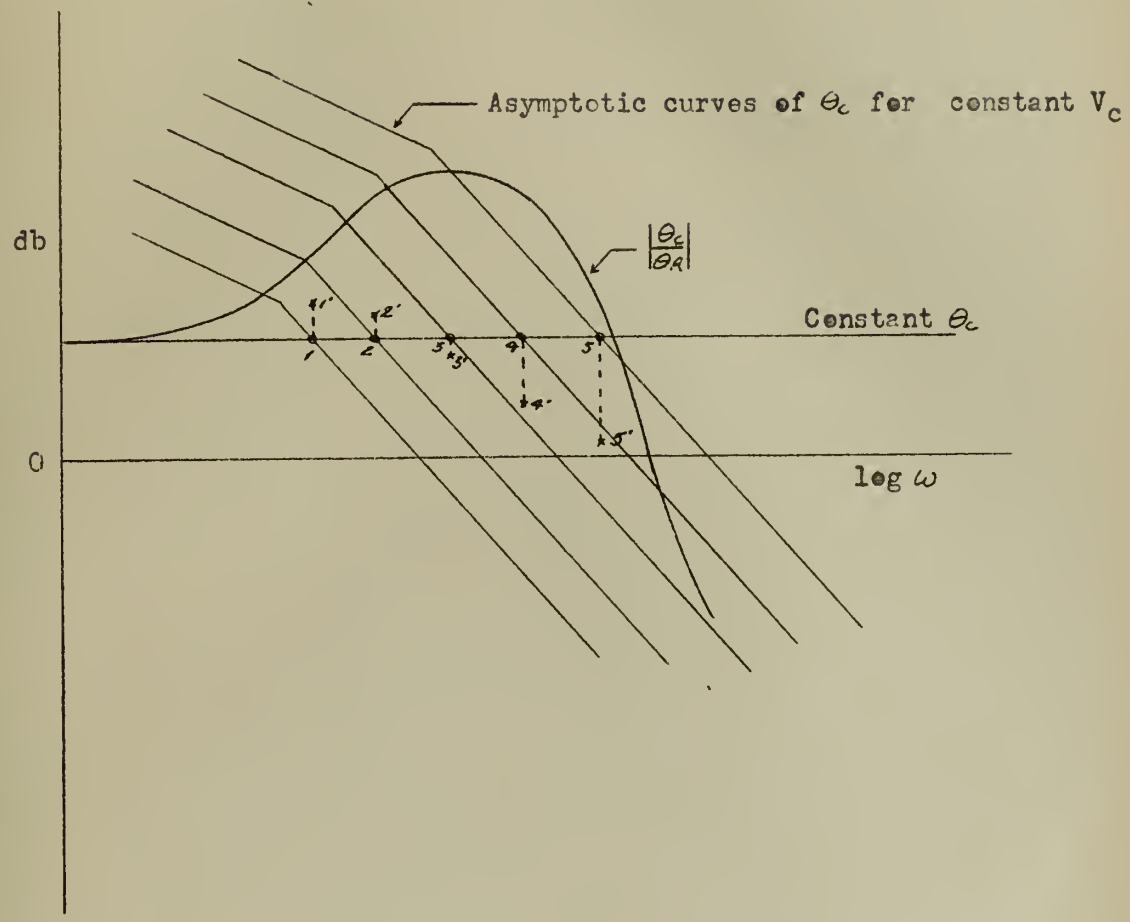

Figure 4. Construction of frequency response for constant θ_c

When using derivative (tachometer) feedback, steps 1, 2, and 3 remain unchanged and the following steps are utilized:

4'. Plot the Bode diagram of $\frac{1}{AF} = \frac{1}{j\omega K_3 + 1}$ and subtract these from points obtained in step 3, including the phase angle points, resulting in a curve of KGAF.

5'. By the Nichols procedure obtain a curve of $\frac{KGAF}{1+KGAF}$ and add to each point the value of 1/AF in both magnitude (decibels) and

phase to obtain the frequency response curve

$$\frac{\Theta_c}{\Theta_R} = \frac{KG}{1+KGAF}$$

for the value of Θ_c chosen.

CHAPTER IV

SOLUTION BY CONSTANT CONTROL FIELD VOLTAGE

A frequency response curve may also be obtained for the condition of a constant control field voltage. This method requires relatively large changes in the magnitude of the input signal, particularly for low values of frequency, hence it is recommended that a Millman adder circuit be used. This method is readily applied to graphical means of predicting the frequency response of a given system. Analytically this method provides relations which are not so readily apparent in the methods previously discussed.

Analytically the procedure is to choose a proper value of control field voltage V_c, and solve equations (5) and (6) or (9) and (10), as the case may be, for various values of ω, which yields the frequency response curve.

In determining the frequency response when either the input or output signal is constant, the amplitude chosen would be representative of the values for which the system is designed. But in using constant V_c the value of V_c which will result in a representative frequency response curve must be estimated.

A study of the variation of θ_c and θ_r is helpful in determining the proper value of V_c. A curve of $|\theta_c|$ for constant V_c may be obtained from equation (4):

$$|\theta_c| = \frac{K_m K_{cT} |V_c|}{\omega \sqrt{\omega^2 \tau_m^2 + 1}} \tag{15}$$

From this equation and equation (5):

$$\left|\frac{\theta_c}{\theta_R}\right| = \frac{K_m K_{CT} K_1}{\sqrt{(K_1 K_m K_{CT} - \omega^2 \tau_m)^2 + \omega^2}} \tag{5}$$

it is found that

$$\theta_R = \frac{V_c}{K_1}\sqrt{\frac{(K_1 K_m K_{CT} - \omega^2 \tau_m)^2 + \omega^2}{\omega^2(\omega^2 \tau_m^2 + 1)}} \tag{16}$$

These equations are plotted in Figure 5.

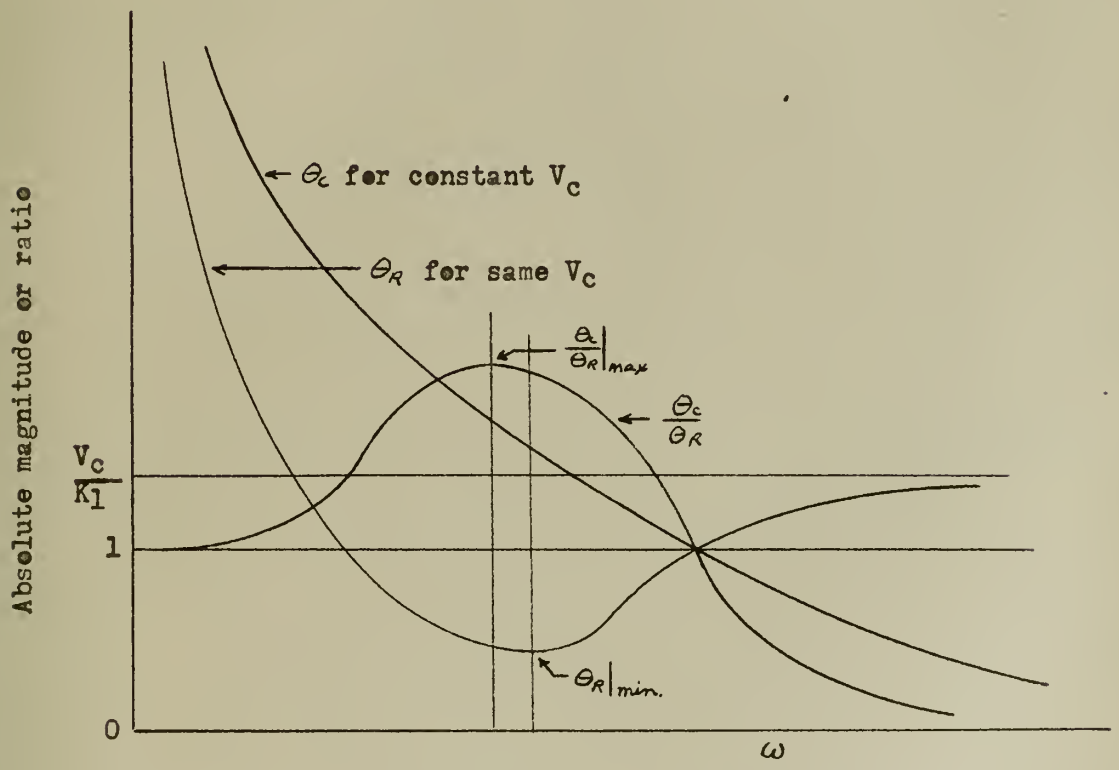

Figure 5. Variation of output and input signals and their ratio for constant control field voltage.

For simplicity let $K = K_1 K_m K_{CT}$. Differentiating equation (16) with respect to ω, the minimum θ_R occurs at

$$\omega^2 = \frac{K\tau_m + \sqrt{(K\tau_m + 1)^2 - 1}}{2\tau_m^2} > \frac{K}{\tau_m} \tag{17}$$

then

$$|\theta_R|_{min} = \frac{V_c}{K_1}\sqrt{\frac{2\tau_m^2K^2 + 4\tau_m K - 2\sqrt{(\tau_m K+1)^2 - 1}\,(\tau_m K-1)}{2\tau_m^2K^2 + 3\tau_m K + \sqrt{(\tau_m K+1)^2-1}\,(2\tau_m K+1)}} \qquad (18)$$

$$|\theta_R|_{min} < \frac{V_c}{K_1}\sqrt{\frac{1}{\tau_m K}} \qquad (18a)$$

Differentiating equation (5) with respect to ω it is found that maximum $\left|\frac{\theta_c}{\theta_R}\right|$ occurs when

$$\omega^2 = \frac{2K-1}{2\tau_m} < \frac{K}{\tau_m} \qquad (19)$$

and then

$$\left|\frac{\theta_c}{\theta_R}\right|_{max} = 2K\sqrt{\frac{\tau_m}{\tau_m + 4K - 2}} \qquad (20)$$

It has been found that for most second order instrument servos using two-phase motors $K > 1 > \tau_m$, hence from equation (20):

$$\left|\frac{\theta_c}{\theta_R}\right|_{max} \doteq \sqrt{K\tau_m} \qquad (20a)$$

It is noted that

$$\omega^2|_{\theta_{R\,min}} > \omega^2\left|_{\left|\frac{\theta_c}{\theta_R}\right|_{max}}\right. \qquad (21)$$

as indicated in Figure 5.

Substituting the value of ω^2 from equation (19), for which $\left|\frac{\theta_c}{\theta_R}\right|$ is maximum, into equation (16) and (15):

$$\theta_R\left|_{\left|\frac{\theta_c}{\theta_R}\right|_{max}}\right. = \frac{V_c}{K_1}\sqrt{\frac{\tau_m + 4K - 2}{(2K-1)[(2K-1)\tau_m + 2]}} \doteq \frac{V_c}{K_1}\sqrt{\frac{1}{K\tau_m}} \qquad (22)$$

$$\theta_c\Big|_{\left|\frac{\theta_s}{\theta_d}\right|_{max}} = \frac{V_c}{K_1} 2K \sqrt{\frac{\tau_m}{(2K-1)[(2K-1)\tau_m+2]}} \doteq \frac{V_c}{K_1} \qquad (23)$$

from which equation (20) is readily obtained.

To obtain a resonance which will correspond to a given input signal, V_c is chosen such that equation (22) is satisfied, which requires some trial and error. On the other hand, if correspondence with a given output signal is desired, V_c is chosen such that equation (23) is satisfied.

The equations developed above may be easily extended to include derivative (tachometer) feedback, resulting in a somewhat more complicated, but straight forward approach.

Once V_c has been chosen the system described by equations (3) or (7) is linear, and linear graphical methods apply.

CHAPTER V

K_m and τ_m

In the preceeding chapters it has been assumed that there exist values of K_m and τ_m such that these relations developed may be applied to nonlinear systems, and that these values are functions of V_c.

It has been shown[2] that K_m and τ_m vary with Vc, and are of a general shape as shown in Figure 6. K_m is determined from steady state operation with V_c constant (unmodulated) and τ_m from a step function transient test, measuring the time required for the system to reach 63.2% of its steady state speed.

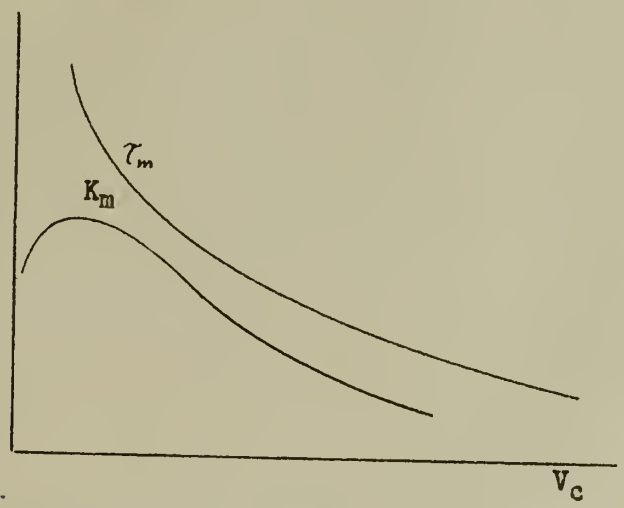

Figure 6. Variation in time constant and gain constant with control field voltage.

The control field voltage actually applied under test is a modulated suppressed carrier wave which, for preliminary investigation, can be considered free of harmonics in both carrier and modulating frequencies. Hence K_m and τ_m vary continuously for a fixed amplitude of modulating frequency, the maximum value of which is hereafter called V_c.

It might be expected that some "average" values of K_m and τ_m exist which can be applied with reasonable accuracy throughout a complete cycle of modulating frequency. As discussed in section 3 of this chapter it is not likely that these "average" values are predeterminable, and it would be adventageous to find representative values of K_m and τ_m in other ways.

1. Determination of τ_m

It was observed that the open loop system under test was not symmetrical in both directions of operation either under steady state operation or when subjected to a step function of small amplitude with all initial conditions zero. It was also noted that reversal of the step after the system had reached constant velocity produced a transient response with time constant other than that obtained when starting from rest. This time constant was dependent on the direction of reversal.

The first phenomenon may be explained on the basis of imperfect symmetry of construction, but the second phenomenon is inherent in the motor. One explanation is that there are indeed two time constants which govern the system; one which obtains when the speed and torque are in the same direction as described[(2)] and one which obtains when the speed and torque have opposite signs.

It is desired, however, to define a single "time constant" which, when applied to the formulae developed, would give favorable results. It seems logical, then, to determine a composite time constant based on a step reversal of control field voltage, defining this time constant as the time required for the system to reach 63.2% of the total change in speed. This time constant is denoted by τ_m.

For the system under test it was found that the time constant as defined above was very nearly constant, the variation being less than the experimental error. It may be concluded that a constant τ_m for the system tested may prove to give good results. This was found to be true, as discussed in the following chapters.

It is entirely possible that the time constant determined as described above may vary with the value of the control field voltage for other systems. Then, when applying the formulae, it is merely necessary to pick the time constant corresponding to the control field voltage under consideration.

2. Determination of K_m.

The gain constant of the motor-load combination (K_m) is well defined[2], which for steady state may be considered to be:

$$K_m = \frac{S}{V_c} \tag{24}$$

where S is speed of the load in radians per second. As the voltage V_c is varied this ratio varies as shown in Figure 6.

It is believed that a good measure of the response of the system is given by the ratio of the maximum value of the modulated output to the maximum value of the modulating input signal, without taking into consideration the actual wave shapes of these signals. The problem, then, is to determine some value of K_m which will provide reasonably good results when dealing with these maximum values.

When a sinusoidal modulating frequency is applied to the control field of a two-phase motor the speed of the motor is not sinusoidal due to the variation in K_m (and τ_m, if τ_m is not constant). In general,

however, the variation in K_m with respect to voltage is less than the rate of change of voltage with respect to time; i. e.,

$$\left|\frac{\partial V}{\partial t}\right| > \frac{\partial K_m}{\partial V} \tag{25}$$

This may also be stated that the product $|K_m V_c|$ never decreases as V_c increases, as illustrated in Figure 7. That is, $|K_m V_c|$ is

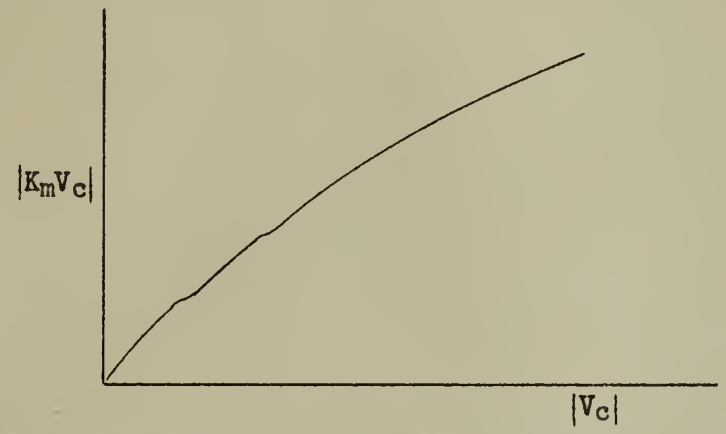

Figure 7. Variation of $|K_m V_c|$ as a function of $|V_c|$.

a single valued and increasing function of $|V_c|$. Thus there will be a one to one correspondence between the maximum speed and the maximum control field voltage, but with a phase lag. It may be concluded that when dealing with the ratios of maximum values of output and input the proper values of K_m to use appears to be the value corresponding to maximum V_c.

It was observed in the system under test that the speed was different in opposite directions of rotation with the same value of applied unmodulated control field voltage. This was particularly noticeable at low values of voltage. Under sinusoidal operation it appears logical to use a value of K_m which is the arithmetic average of those obtained from

opposite directions of rotation.

Under steady state single loop operation the control field voltage will not be sinusoidal since it is composed of a combination of sinusoidal input and non-sinusoidal output; nevertheless the maximum value of this non-sinusoidal voltage corresponds to the maximum value of the non-sinusoidal output. This was found to be in agreement with experimental results, as discussed in chapter VI.

3. Some considerations on wave shapes.

Besides the harmonics in the modulating frequency due to the variation of K_m (and τ_m, if not constant), the shape of the modulating frequency is also affected by other factors:

a. Neglecting harmonics in the carrier frequency wave the tachometer output may be considered to be composed of two waves: one which is proportional to the speed of the tachometer and one which is due to transformer action between the two windings which are not precisely in quadrature. The net result is a modulated carrier output which is non-symmetrical both in time and magnitude. This can be shown by a vector diagram of a modulated suppressed carrier wave as illustrated in Figure 8a.

In this figure the vector representing the voltage due to transformer action does not rotate with respect to the coordinates (which are rotating at carrier frequency). The resulting envelope of the modulated wave is shown in Figure 8b, and it is apparent that when using tachometer feedback the wave shape of the output voltage is affected.

It is depicted in Figure 8 that the resultant speed voltage and the voltage due to transformer action are in phase (or 180° out of phase,

depending on their position). This is not necessarily true, but the resulting action is as explained.

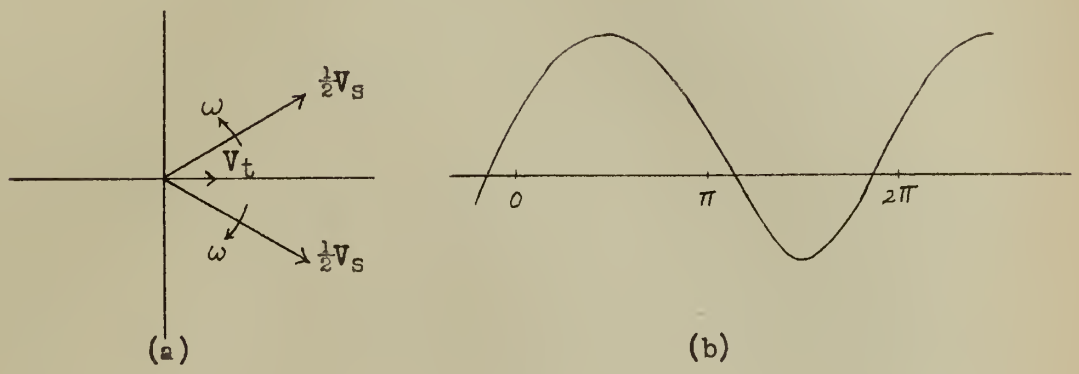

Figure 8. (a) Vector diagram and (b) wave shape of tachometer output. V_s - voltage due to speed of tachometer
V_t - voltage due to transformer action
ω - modulating frequency

The variation of the magnitude of the transformer action voltage with speed is very small, and may be considered constant. Its effect is thus most noticeable at low speeds; i. e., low values of control field voltage.

b. It has been noted above that the speed of the motor was different in opposite directions of rotation with the same value of applied control field voltage. Hence when using tachometer feedback the wave shape of the output voltage will be altered by the fact that the tachometer itself is not turning with equal speeds in both directions.

c. Details of the physical construction of the electrical components of the system such as slots and teeth, non-symmetrical air gaps, etc., cause ripples to be introduced in the output wave shape. These are particularly noticeable at low values of control field voltage. The

frequency of these ripples is dependent on the speed of operation.

d. The wave-shape is also affected by backlash, coulomb friction, and stiction which are inherent in any electro-mechanical system.

e. Harmonics of carrier frequency affect the modulating frequency wave shape. These harmonics are introduced primarily in the tachometer and control transformer.

It was previously noted that there may exist some mathematically derived "average" values of K_m and τ_m which may be applied with reasonable accuracy throughout a complete cycle of modulating frequency. The wave shape of the control field voltage under actual test conditions, however, departs appreciably from a sine wave. It is almost impossible to predict the wave shapes to be encountered, hence the possibility of finding such average values is very remote. Some typical wave shapes are found in Appendix B.

CHAPTER VI

EXPERIMENTAL VERIFICATION

In order to verify the theory developed in the preceeding chapters some points on the frequency response curves for constant input and variable error signal gain were checked experimentally. The experimental procedure is discussed in the following chapter. The gain of the amplifier in use varied somewhat with the magnitude of the input to the amplifier, making it very difficult to maintain constant error signal gain throughout the frequency range. Consequently only one complete frequency response curve for a particular gain is given. These results are given in Figure 9, where the experimental points are indicated on the computed curve.

For other values of error gain isolated points were checked. The results are shown in Table I.

It is seen that in the range of interest the agreement between experimental and computed results is very good; in fact, well within the limits of experimental accuracy. It is noted that at low values of control field voltage the agreement is not so good as at higher values. This is due to the additional nonlinearities of the system, discussed in Chapter V, which are particularly apparent at low voltages.

As to the frequency response under the other two conditions, namely constant θ_c and constant V_c, there is no reason to believe the computed and experimental values will not agree. Isolated points were checked from the experimental data obtained with constant θ_R, with good results.

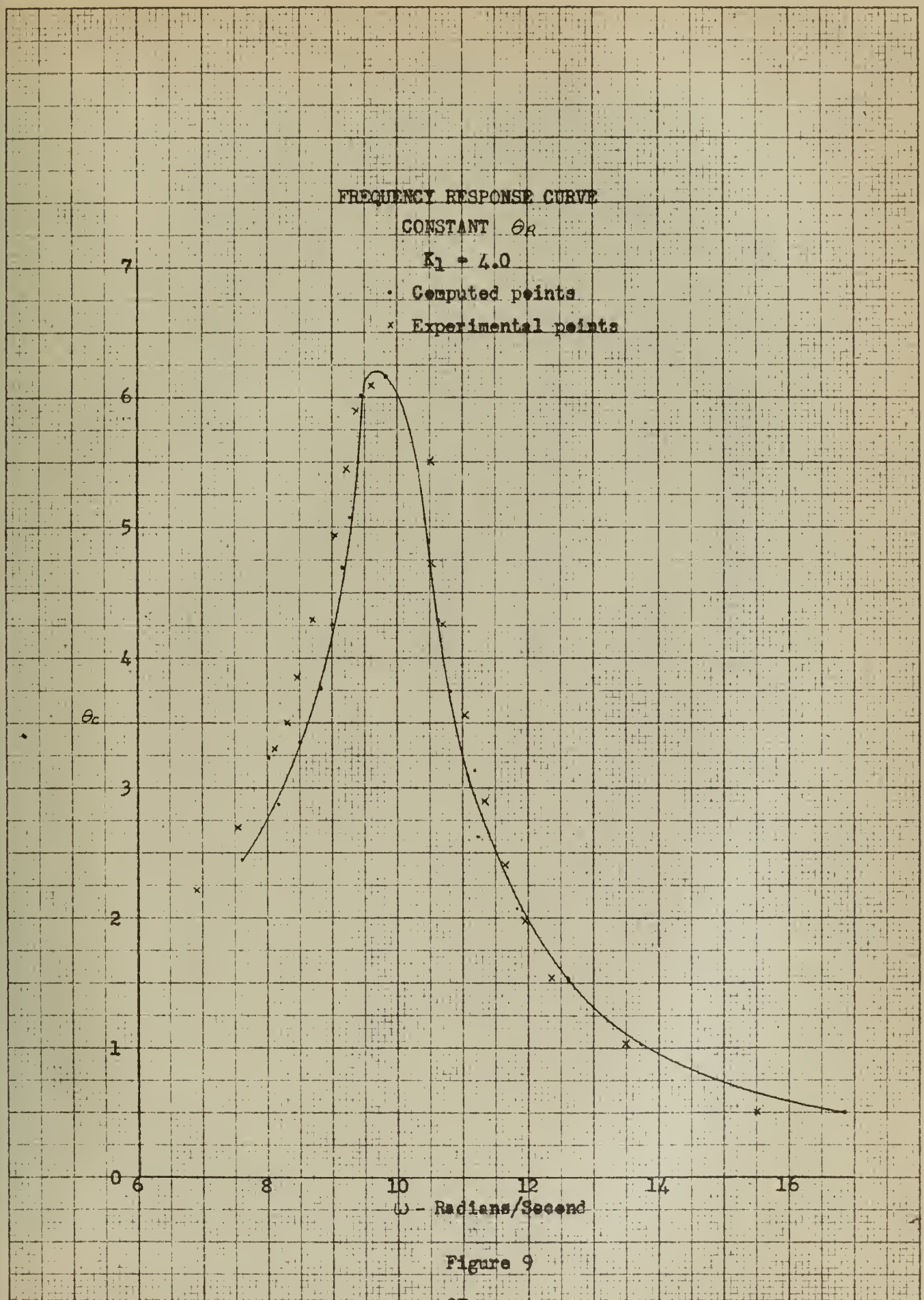
FREQUENCY RESPONSE CURVE
CONSTANT θ_R
$K_1 = 4.0$
· Computed points
× Experimental points
θ_c
0
1
2
3
4
5
6
7
6
8
10
12
14
16
ω - Radians/Second

Figure 9

TABLE I

Individual frequency response points, $\theta_R = 1$

K_1	Computed points			Experimental points		
	ω	θ_c	$\angle \frac{\theta_c}{\theta_R}$	ω	θ_c	$\angle \frac{\theta_c}{\theta_R}$
4.92	7.45	1.887	11.7	6.56	1.8	3.0
5.54	7.99	2.01	11.7	7.32	1.87	5.0
5.44	8.50	2.165	13.7	8.03	2.05	7.0
6.0	9.40	2.46	15.2	8.65	2.40	
5.79	9.75	2.74	18.2	9.25	2.7	15
5.58	10.05	3.50	24.9	9.90	3.4	18
5.85	10.61	4.19	24.8	10.42	4.1	23
6.00	11.11	5.14	32.8	10.86	5.1	35
6.11	11.35	6.28	58.5	11.20	6.5	51
5.75	11.25	7.26	90	11.70	7.5	89
5.89	11.42	6.90	90	12.02	6.7	113
6.17	12.50	5.25	128.7	12.44	5.15	131
5.85	13.42	3.56	153.0	12.90	4.0	150
5.80	13.42	3.00	151.3	13.10	3.05	161
5.87	13.70	2.39	157.7	13.50	2.20	168
6.03	16.05	1.328	166.2	14.32	1.43	174
5.90	17.52	.889	169.7	15.96	1.05	177
5.97	19.90	.609	172.1	18.40	.8	178

CHAPTER VII

EXPERIMENTAL METHODS

1. Servomechanism

In order to measure and verify the quantities appearing in the preceeding chapters a typical instrument servomechanism was assembled. A block diagram of the motor-load portion of the system appears as in Figure 10.

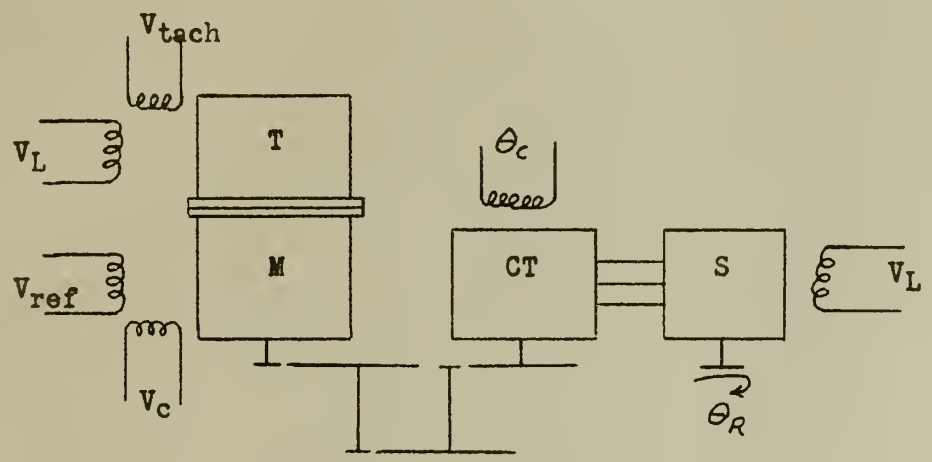

Figure 10. Motor-load portion of servomechanism
M Two phase motor
T Two phase AC tachometer
CT Control transformer
S Synchro

2. Determination of τ_m and K_m.

The method described[2] was employed in determining K_m and τ_m of the system with the exception that a step reversal of the control field voltage was used to determine τ_m, as explained in Chapter V. The block diagram for these measurements is shown in Figure 11. This circuit was used instead of merely applying quadrature voltages to the motor in order

to approximate the actual operating conditions for determining the frequency response. The reversing switch was placed between the amplifier and the matching transformer in order to take into consideration any response time which might exist in other portions of the system.

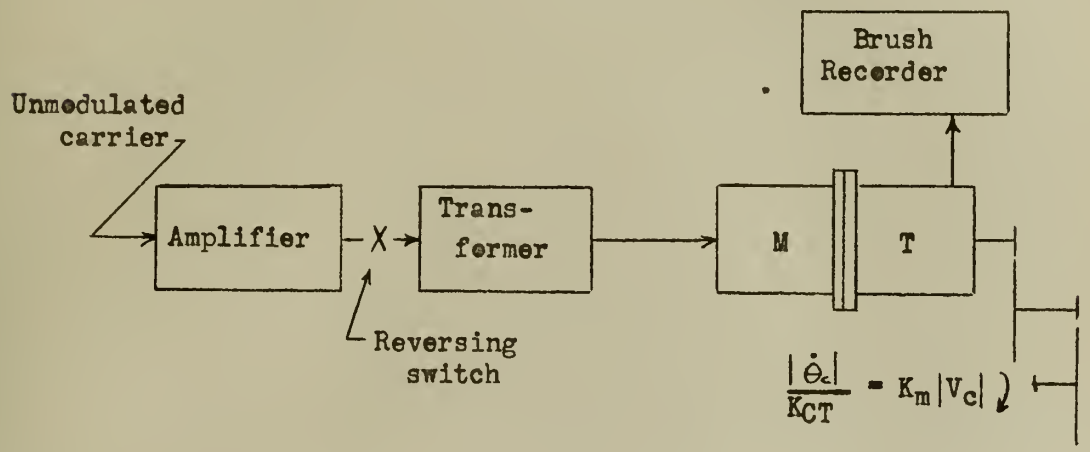

Figure 11. Block diagram of system for measurement of τ_m and K_m.

To measure the transient response for a step reversal the output of the tachometer was recorded on a Brush recorder. The desired time constant is the time required for the system to reach 63.2% of the total change in speed with a V_c peak to peak applied to the motor equal to the V_c under consideration. (Recall that maximum values are used.) This is indicated in Figure 12.

The gain constant (K_m) was determined by stop watch measurement of the speed of the load, averaged for operation in both directions. As noted in Figure 11, this speed may be interpreted as

$$\frac{|\dot{\theta}_c|}{K_{CT}} = K_m|V_c| \tag{26}$$

from which K_m may be calculated.

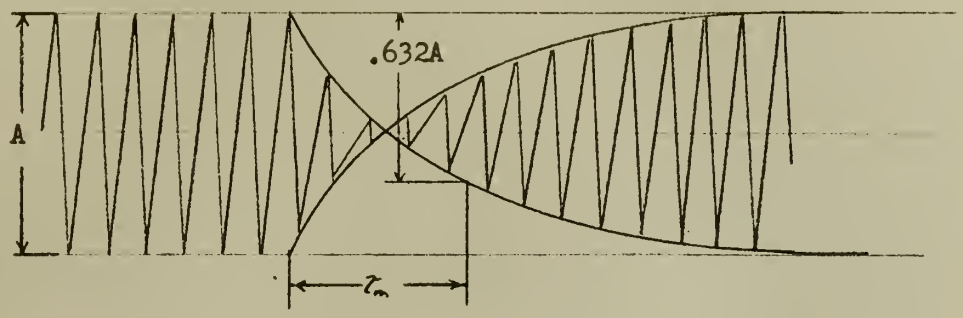

Figure 12. Determination of time constant.

The resulting curves of K_m and τ_m vs. V_c are shown in Figure 13.

3. The basic block diagram used for determination of frequency responsee is shown in Figure 14. Various types of adder circuits may be employed as explained below. The adder circuit must be such that its output, which is the input to the amplifier, is directly proportional to the error signal, which, from Figure 1, is

$$\theta_R - \theta_c - \frac{K_s}{K_{cT} N} j\omega\theta_c \qquad (27)$$

when the input is proportional to each of these quantities. This may be accomplished in either of two ways: a series adder or a Millman (parallel) adder.

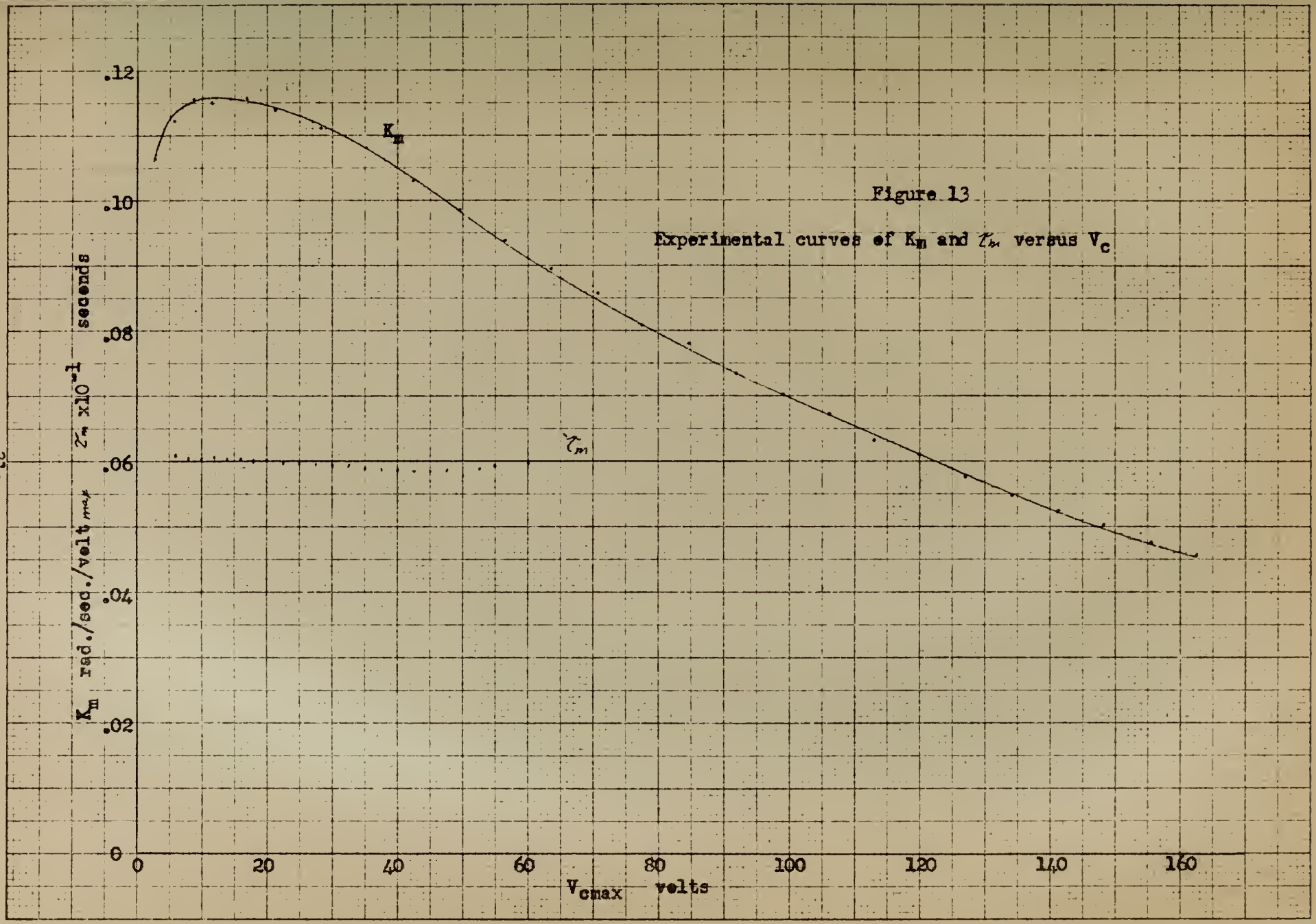

Figure 13

Experimental curves of K_m and τ_m versus V_c

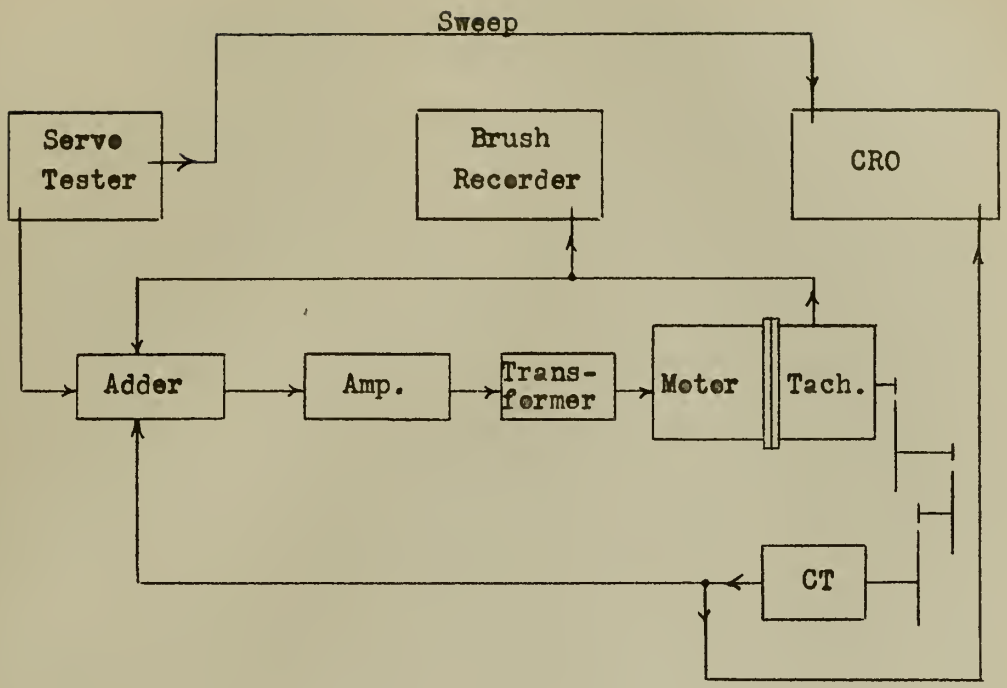

Figure 14. System block diagram as used for frequency response determination.

The series adder, shown in Figure 15, is the simplest circuit, and is preferable when the maximum output of the tester is sufficient to obtain the desired conditions.

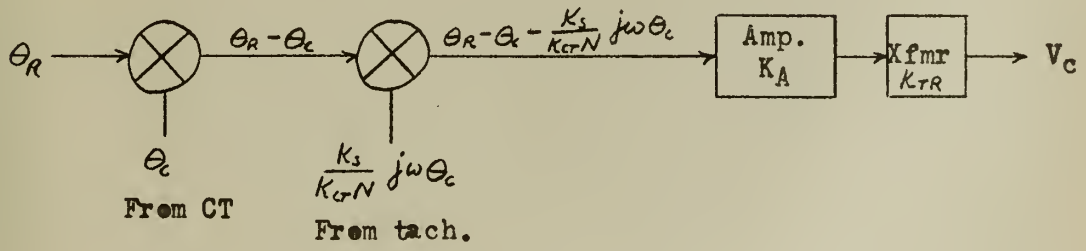

Figure 15. Series adder circuit.

From the circuit of Figure 15,

$$V_c = K_A K_{TR} \left[\theta_R - \theta_c - \frac{K_s}{K_{cr} N} j\omega\theta_c\right] \tag{28}$$

The error signal gain, in this case is

$$K_1 = K_A K_{TR} \tag{29}$$

which should be maintained constant during a frequency response determination for conditions under consideration. This may be accomplished by proper selection of the amplifier and matching transformer.

It often occurs that the output of the tester is insufficient in magnitude to obtain the desired conditions. Larger command signals may be obtained by properly amplifying the tester signal. It is difficult to obtain an amplifier, however, in which the phase shift of the carrier is independent of the magnitude of the applied signal. Since the sinusoidal test signal is constantly varying, the phase of the carrier would continuously shift with such an amplifier.

Larger command signals may also be simulated by use of a Millman (parallel) adder circuit, shown in Figure 16. From this figure, and

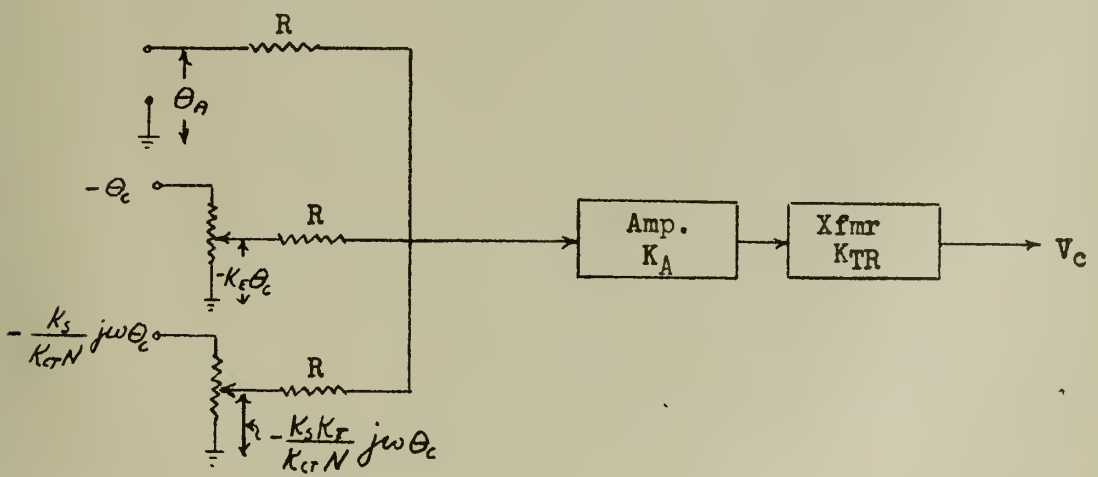

Figure 16. Millman adder circuit.

as derived in Appendix A,

$$V_c = \frac{K_A K_{TR} K_E}{3}\left[\frac{\theta_A}{K_E} - \theta_c - \frac{K_S K_T}{K_E K_{cT} N} j\omega\theta_c\right] \tag{30}$$

where, by definition, $\theta_R = \frac{\theta_A}{K_E}$. It is seen that by varying K_E large values of command signal, θ_R , may be simulated.

The error signal gain is

$$k_1 = \frac{K_A K_{TR} K_E}{3} \tag{31}$$

which should remain constant for any particular desired condition of frequency response. This may be accomplished with a properly selected amplifier with adjustable gain control. It is noted that the amount of tachometer feedback is also varied by a variation in K_E. If it is desired to maintain a constant value of tachometer feedback the ratio $\frac{K_T}{K_E}$ must be maintained constant.

If the tester frequency indicator is not sufficiently accurate for the desired purpose, the frequency may be obtained from a time recording of the output of the tachometer, control transformer, or tester. It is noted that the frequency must be determined with considerable accuracy. The greater the recording time the greater the accuracy. In general, servo testers have provisions for measuring the phase shift of θ_c with respect to θ_R with sufficient accuracy.

The procedure for obtaining the frequency response with constant θ_R is self-evident and is not discussed here.

Under the condition of constant θ_c the procedure is to set the frequency, then vary the amplitude of the command signal, θ_R , to obtain the

desired θ_c . This presents no problem when using the series adder circuit. When using the Millman adder circuit and θ_R is varied by adjusting K_E (which is necessary if the tester output is not sufficiently large for the desired purpose), the amplifier gain must be reset with each change in K_E in order to maintain constant error signal gain. Even without tachometer feedback this is a cumbersome procedure since two controls must be adjusted simultaneously to maintain both θ_c and K_1 constant. The problem is further multiplied when using tachometer feedback in that K_T must also be varied simultaneously in order to maintain constant $\frac{K_T}{K_E}$.

After adjustment of these controls the value of the resulting command signal may be found by measuring θ_A and K_E, computing $\theta_R = \frac{\theta_A}{K_E}$.

A similar procedure is used to obtain the frequency response under conditions of constant V_c, except that θ_R is now varied to obtain the desired V_c, measuring the resulting θ_R and θ_c .

CHAPTER VIII

CONCLUSIONS

1. The effect of the nonlinearity of a two phase motor on the frequency response of a servomechanism using this motor may be computed by analytical and graphical methods.

2. The numerical results of such calculations are sufficiently accurate for engineering purposes as demonstrated by a comparison of experimental and computed results.

3. The specific computational methods described in this thesis are more general than implied by the immediate problem considered. They may be extended to any similar system in which there are parameters having nonlinear variation similar to K_m and τ_m .

4. The general principle used in the derivation of the calculations is applicable to many other nonlinear problems. This principle may be stated as follows:

> The frequency response of a nonlinear system may be computed to engineering accuracy by considering that the nonlinear differential equation of the system may be linearized at each value of frequency used in the computations. The linearization procedure consists of determining a set of numerical parameters which may be considered constant at the stated frequency, but which, in general, will differ from the values of these parameters at any other frequency.

5. At present the frequency response found by these methods cannot be correlated to the transient response by methods normally used in linear systems.

The immediate problem is to devise some means of correlating the frequency response of a nonlinear system to its transient response for both a step and ramp input, using similar mathematical techniques. This is recommended as a topic for further investigation.

BIBLIOGRAPHY

1. Stallard, D. V. — A Series Method of Calculating Control-System Transient Response from the Frequency Response, AIEE Trans., part II, Mar. 55, pp 61-64

2. Stein, W. A. and Thaler, G. J. — Evaluating the Effect of Nonlinearity in a Two Phase Servomotor, AIEE Trans., part II, Jan. 55, pp 518-521.

3. Thaler, G. J. — Elements of Servomechanism Theory, (book), McGraw Hill, 1955. (McGraw Hill Electrical and Electronic Engineering Series)

4. James, H. M., Nichols, N. B., Phillips, R. S. — Theory of Servomechanisms (book), McGraw Hill, 1947. (MIT Radiation Laboratory Series, Vol 25)

5. Seely, S. — Electron Tube Circuits (book), McGraw Hill, 1955. (McGraw Hill Electrical and Electronic Engineering Series)

APPENDIX A

DERIVATIONS

1. Equations for a linear system.

The motor-load portion of a typical servomechanism may be shown schematically as in Figure 17. The symbols represent quantities

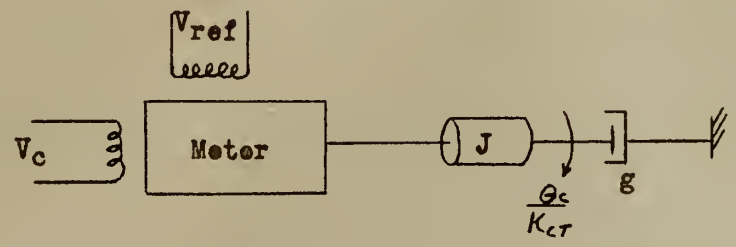

Figure 17. Schematic representation of motor-load portion of a typical servomechanism.

which are:

J Equivalent moment of inertia of entire electromechanical portion of the system, with dimensions ML^2.

g Equivalent damping coefficient of the entire electromechanical portion of the system composed of two terms: the viscous friction, f, and the torque damping term, $\frac{\partial T_o}{\partial \theta_c}$, where T_o is the torque developed by the motor. The dimensions of g are ML^2T^{-1}.

K Torque constant of the motor with dimensions ML^2T^{-2}/volt.

$\frac{\theta_c}{K_{cT}}$ Position of the load, which is dimensionless (radians).

Consider this system to be linear; i. e., g and K are constants. The linear differential equation of this system is then:

$$J\frac{\ddot{\theta}_c}{K_{cT}} + g\frac{\dot{\theta}_c}{K_{cT}} = KV_c \qquad \text{(A-1)}$$

By methods of Laplace transforms

$$\frac{\theta_c(s)}{K_{cT}} = \frac{\frac{K}{g}V_c(s)}{s\left(\frac{J}{g}s+1\right)} \qquad \text{(A-2)}$$

By definition, the gain constant of the motor-load combination is

$$K_m = \frac{K}{g} \qquad \text{(A-3)}$$

with dimensions (radians)-T^{-1}/volt. The time constant of the motor-load combination is

$$\tau_m = \frac{J}{g} \qquad \text{(A-4)}$$

with dimension T.

Substitution of equation (A-3) and (A-4) in equation (A-2),

$$\frac{\theta_c(s)}{K_{cT}} = \frac{K_m V_c(s)}{s(s\tau_m+1)} \qquad \text{(A-5)}$$

In linear systems the complex form of this equation when a sinusoidal voltage is impressed on the control field may be obtained from the transformed equation by replacing s by $j\omega$. Then

$$\theta_c = \frac{K_m K_{cT} V_c}{j\omega(j\omega\tau_m + 1)} \qquad (1)$$

The transfer function of the motor-load combination for a system such as shown in Figure 17 is

$$\frac{\theta_c}{V_c} = \frac{K_m K_{cT}}{j\omega(j\omega\tau_m + 1)} \qquad (A\text{-}6)$$

The inertia and damping of the tachometer has been included in these terms for the motor-load combination for the system, hence it is assumed that the output of the tachometer is directly proportional to its speed, or

$$\text{tachometer output} = K_s \frac{\dot{\theta}_c}{K_{cT} N} \qquad (A\text{-}7)$$

where K_s is the tachometer constant in T^{-1}volts. Since the tachometer is mounted on the motor shaft and the output position of the system is considered to be that of the load, the speed ratio of load/motor must appear in this expression. In complex form for sinusoidal V_c, equation (A-7) is

$$\text{tachometer output} = \frac{K_s}{K_{cT} N} j\omega\theta_c \qquad (A\text{-}8)$$

Defining K_1 as the error signal gain constant, it follows from Figure 1 that

$$V_c = K_1\left(\theta_R - \theta_c - \frac{K_s}{K_{CT}N} j\omega\theta_c\right) \qquad \text{(A-9)}$$

The direct transfer function of the amplifier and motor-load combination is then

$$KG = \frac{K_1}{V_c}\theta_c = \frac{K_1 K_m K_{CT}}{j\omega(j\omega\tau_m + 1)} \qquad (2)$$

or

$$KG = \frac{\theta_c}{\theta_R - \theta_c - \frac{K_s}{K_{CT}N} j\omega\theta_c} \qquad \text{(A-10)}$$

The system function or frequency response function, defined as $\frac{\theta_c}{\theta_R}$, and where $K_3 = K_s/K_{CT}N$, is

$$\frac{\theta_c}{\theta_R} = \frac{\frac{K_1 K_m K_{CT}}{j\omega(j\omega\tau_m + 1)}}{1 + \frac{K_1 K_m K_{CT}}{j\omega(j\omega\tau_m + 1)} + K_3 j\omega \frac{K_1 K_m K_{CT}}{j\omega(j\omega\tau_m + 1)}} \qquad \text{(A-11)}$$

$$= \frac{\frac{K_1 K_m K_{CT}}{j\omega(j\omega\tau_m + 1)}}{1 + \frac{K_1 K_m K_{CT}}{j\omega(j\omega\tau_m + 1)}\left(j\omega K_3 + 1\right)} \qquad (7)$$

It is seen that if K_3 is zero (without tachometer feedback), equation (7) reduces to equation (3).

Manipulation of equation (7) yields

$$\frac{\theta_c}{\theta_R} = \frac{K_1 K_m K_{cT}}{K_1 K_m K_{cT} - \omega^2 \tau_m + j\omega(1 + K_1 K_3 K_m K_{cT})} \qquad \text{(A-12)}$$

from which the magnitude and angle may be obtained

$$\left|\frac{\theta_c}{\theta_R}\right| = \frac{K_1 K_m K_{cT}}{\sqrt{(K_1 K_m K_{cT} - \omega^2 \tau_m)^2 + \omega^2(1 + K_1 K_3 K_m K_{cT})^2}} \qquad (9)$$

$$\tan \angle \frac{\theta_c}{\theta_R} \qquad \frac{-\omega(1 + K_1 K_3 K_m K_{cT})}{K_1 K_m K_{cT} - \omega^2 \tau_m} \qquad (10)$$

which reduce to equations (5) and (6) if K_3 is zero.

The extension of these equations to nonlinear systems is found in the body of the thesis.

2. Millman adder circuit.

It has been developed[5] that in a circuit of the form shown in Figure 18, where the voltages are measured from the same reference, the voltage E is given by

$$E = \frac{E_1 Y_1 + E_2 Y_2 + E_3 Y_3}{Y_1 + Y_2 + Y_3} \qquad \text{(A-13)}$$

or, in general,

$$E = \frac{\sum E_s Y_s}{\sum Y_s} \qquad \text{(A-14)}$$

This is easily shown by applying Kirchoff's Laws.

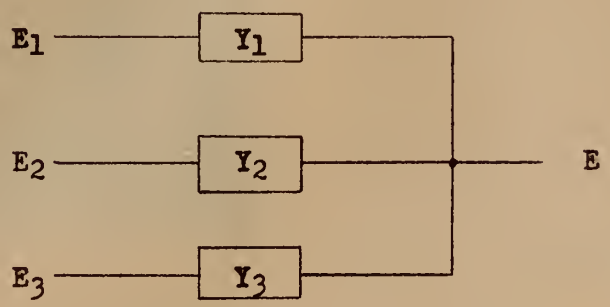

Figure 18. Millman adder circuit.

APPENDIX B

WAVESHAPES

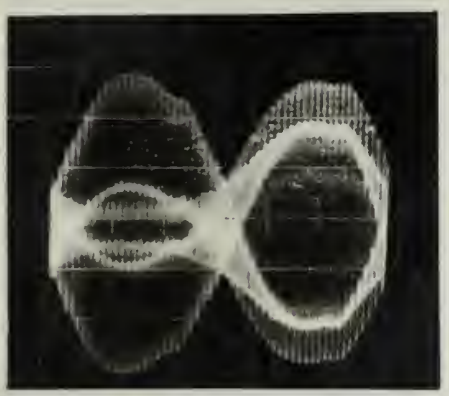

The waveshapes shown at left are the input signal, θ_R; output signal, θ_C; and control field voltage, V_c, respectively, for low frequency and low value of control field voltage, without tachometer feedback. Effects of harmonics, as discussed in section 3 of Chapter V, are plainly visible. The input signal is a sine wave.

Data for these waveshapes are:

θ_R = 1 volt max

θ_C = 1.25 volts max

V_c = 4.9 volts max

ω = 7.85 rad/sec.

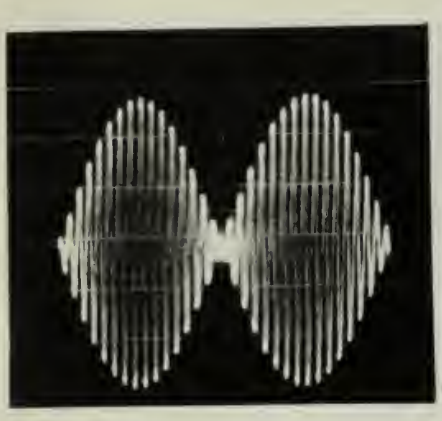

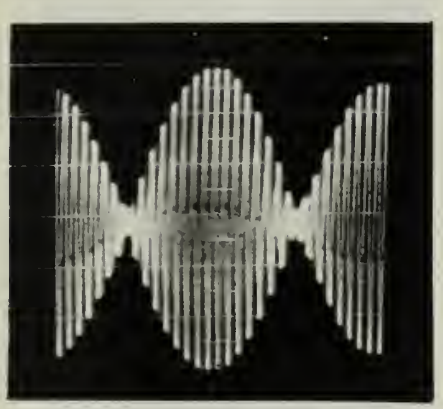

The waveshapes shown at left are, respectively, the input signal, θ_{i2}; the output signal, θ_c; and the control field voltage, V_c, without tachometer feedback, with the system operating near the resonance point. The effect of harmonics is almost negligible. The phase angle of θ_c with respect to θ_{i2} is seen to be about 90°. The input signal is a sine wave.

Data for these waveshapes are:

θ_{i2} = 1 volt max

θ_c = 6.6 volts max

V_c = 36 volts max

ω = 11.83 rad/sec.

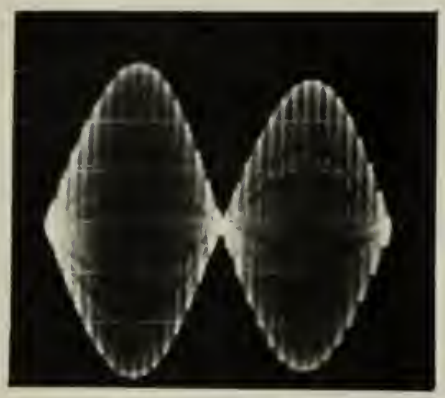

It was noted in section 3 of Chapter V that the output of the tachometer was unsymmetrical in both time and magnitude, which is evident from the waveshape at top left. The left center picture shows the waveshape of the tachometer carrier signal.

The output carrier signal is shown in the lower two photographs. The left hand picture is of a large signal (6 volts max) and the right picture for a small signal (2 volts max). The third harmonic is very evident in this picture.

APPENDIX C

MISCELLANEOUS ITEMS

1. Data on equipment

   a. Motor-generator: Kollsman type 890-0160600 ser 2954.

   b. Control Transformer: Type 1HCT Mk 11 Mod 4 ser 1998. Ord Dwg 950501.

   c. Synchro Motor: Type 1F Mk 8 Mod 1 ser 8273. Ord Dwg 212871-1 115/90 volts.

   d. Matching Transformer: Standard Transformer Corp. part #A-3851.

   e. Servo Tester: Industrial Control Co. Dynamic Analyzer type 100-A ser 72.

2. The circuit diagrams for the amplifiers used in amplifying the error signal are shown in Figures 19 and 20. The gain of these amplifiers is nominally constant for 60 cycles per second within the range of operation.

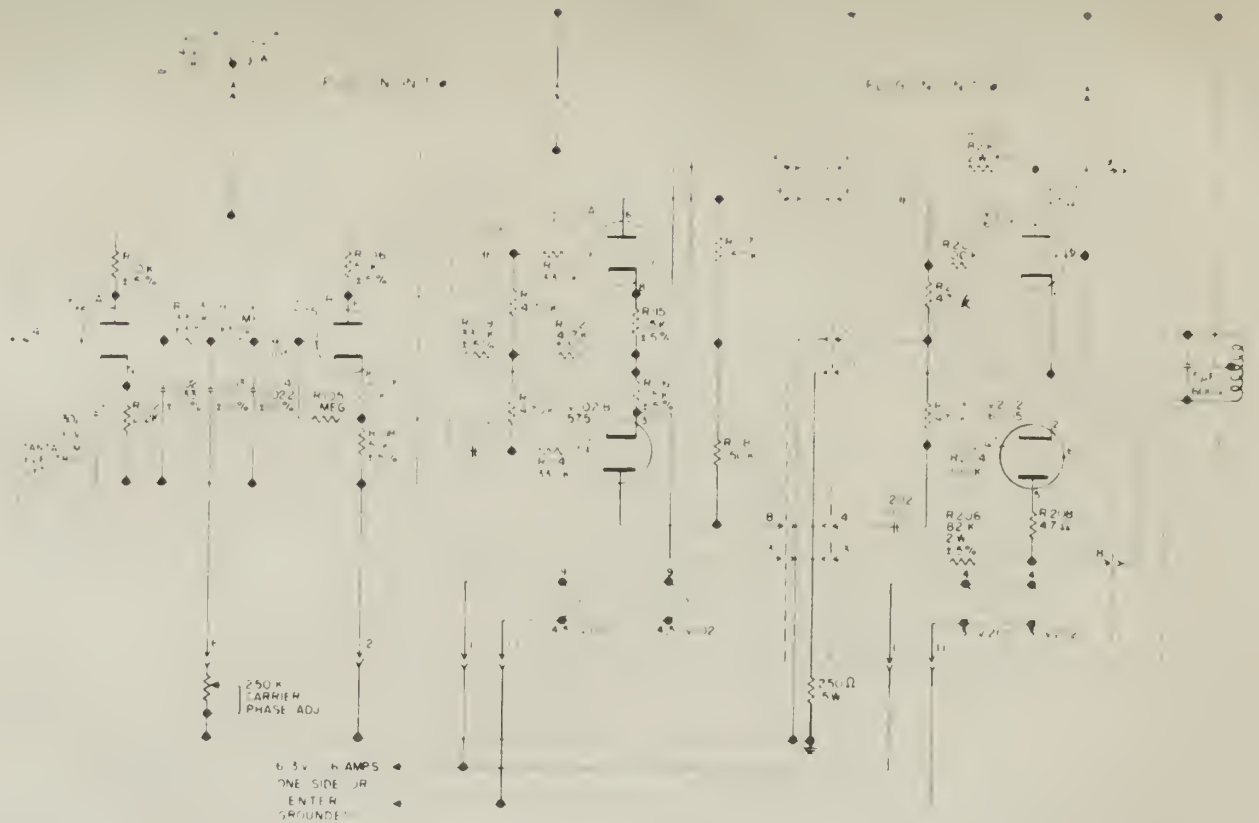

NOTES

1 ALL RESISTORS ARE ½ WATT, ±10% EXCEPT AS NOTED
2 ALL CAPACITORS ARE 400 V, ±20% EXCEPT AS NOTED
* DECOUPLING NOT REQUIRED WITH WELL REGULATED POWER SUPPLY

Figure 19. NEL Unitized Servo Amplifer

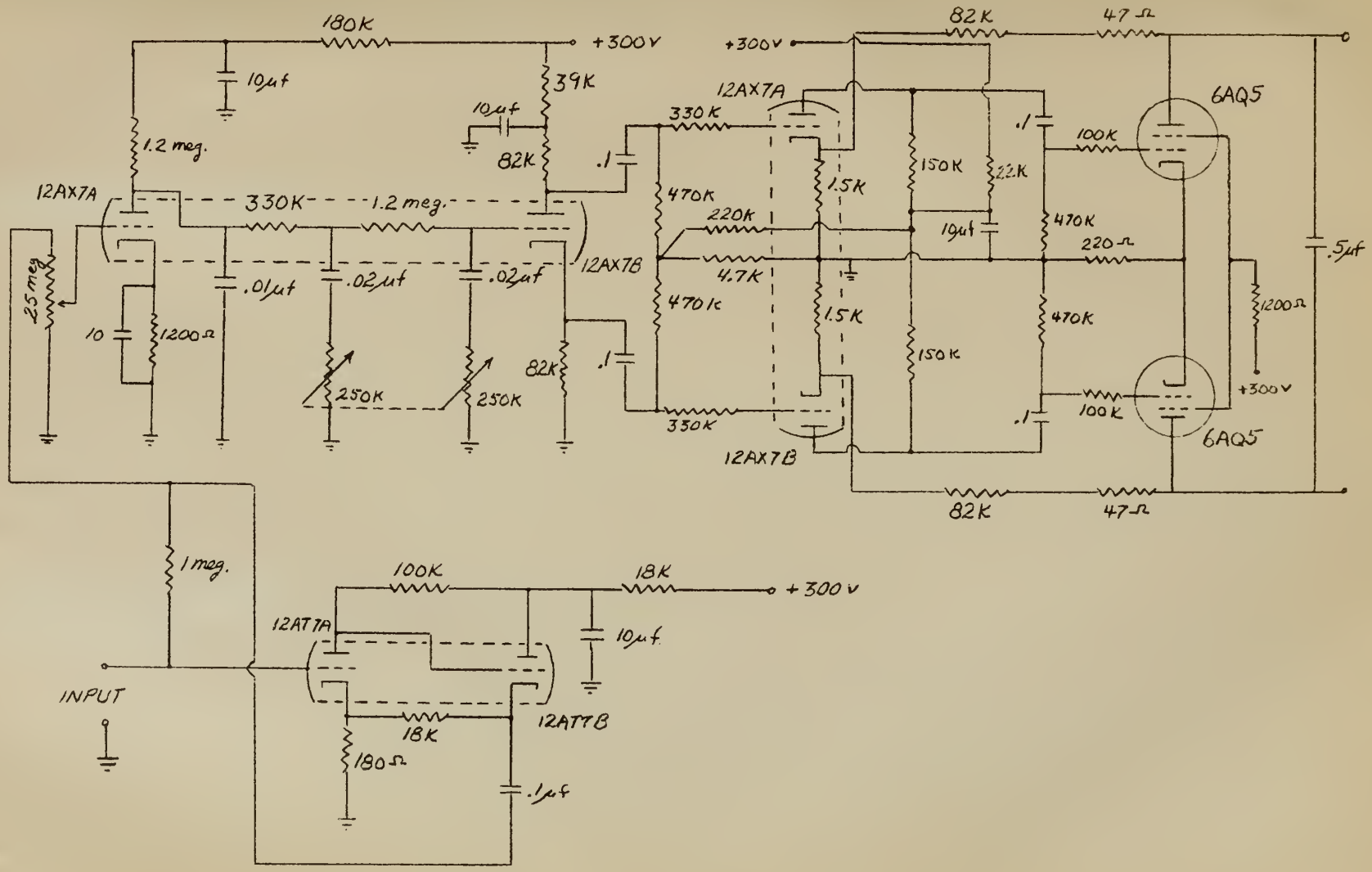

Figure 20. Modified NEL Servo Amplifier